Egyptian Journal of Chemistry

http://ejchem.journals.ekb.eg/

Synthesis of functionalized magnetite nanoparticles for wastewater treatment

Naema S. Yehia[1], Farag A. Issa[1], Mohamed ElAzab[1], Abdelrahman A. Badawy [2,*]

[1]. Chemistry Department, Faculty of Science, Menofiya University, Shebein El-Kom, Egypt

2. Physical Chemistry Department, Advanced Materials Technology and Mineral Resources Research Institute, National Research Centre, 12622, Giza, Egypt

Abstract

A Series of magnetite (Fe_3O_4) nanocomposite based efficient photocatalysts was synthesized employing coprecipitation method. Characterization of pure and different coated samples was achieved by using XRD, IR, specific surface area (S_{BET}) and SEM techniques. The results revealed that the formation of the magnetite crystal without any impurities. The SEM images of this catalyst exhibited regular well crystalline microstructures with almost spherical shape and homogenous particle size in the range of nano scale. The presence of sodium lauryl ether sulfate (SLES) resulted in an increase in crystallinity. This increase led to a decrease in both of the particle size and the spherical shape regularity; however the particles boundary is still preserved. The as-prepared samples recorded photocatalytic activities towards degradation of organic pollutants in waste water. The sample coated with SLES displays the highest activity (with 90.1% efficiency in 180 min) due to the role of SLES.

.

Keywords: Magnetite nanoparticles, Polyphenols of tannins, Coprecipitation, Water treatment, SLES

1. Introduction

We are aware that water is crucial to the survival of all living things and plays a significant economic role. A variety of industrial processes and other economic activities depend on water. Due to the increasing levels of pollutants brought into the water from a variety of sources, Surface water quality is significantly impacted by human activity [1]. Due to the high concentrations of organics and nutrients in untreated municipal wastewater, it has been deemed to be the most harmful to water ecosystems [2]. A number of chemical, physical, and biological procedures can be used to treat wastewater [3–4]. The most effective technique for treating process or waste effluents to remove colours, smells, oils, and organic contaminants was adsorption because of its straightforward construction, low initial cost, and simplicity of use [5]. There has been a lot of study done on adsorbents that are effective and cheap. The sorbents that have been documented include clay, zeolites, siliceous minerals, industrial waste, agricultural waste, and biosorbents including chitosan and peat [6, 7].

Several studies have been concerned iron oxide nanoparticles for the removal of chemical sorts like gases, metals, and dyes as it has low diffusion resistance and a large surface area [7- 9]. Numerous reviews elsewhere were focused on the preparation of magnetic nanoparticles with suitable morphology, tailored properties, and a fine size distribution [14-16]. The co-precipitation technique [17:19], the hydrothermal treatment [20-22], the oxidative hydrolysis [23, 24], and the thermal decomposition of iron-containing molecular are all examples of colloidal magnetite nanoparticle synthesis methods.

The most common method, co-precipitation, is one of the simplest and most efficient ways to produce controlled-size magnetite nanoparticles [28]. The co-precipitation method produces magnetic Fe_3O_4 nanoparticles by aging stoichiometric mixtures of ferric and ferrous hydroxides in an aqueous solution [29]. The precipitation reaction typically involves mixing Fe^{2+} and Fe^{3+} in a molar ratio of 1:2, which is the exact stoichiometry for Fe_3O_4 [30]. For complete precipitation, a pH range of 8 to 14 is required. As shown in Equation (1), the method's reaction mechanism is:

$$Fe^{2+} + Fe^{3+} + 8\ OH^- \leftrightarrow Fe(OH)_2 + 2Fe(OH)_3 \rightarrow Fe_3O_4 + 4H_2O \quad \ldots\ldots\ldots\ldots (1)$$

At the laboratory scale, magnetic nano-adsorbents are emerging as remarkable functional materials

*Corresponding author e-mail: aabadawy11@gmail.com

Receive Date: 18 February 2023, Revise Date: 10 March 2023, Accept Date: 14 March 2023

DOI: 10.21608/ejchem.2023.191227.7547

with excellent ability to sequester micro-pollutants and fast adsorption kinetics [31-41]. Most of the time, magnetic nano-adsorbents have a lot of specific surface areas and a lot of interconnected porous networks [42, 43] that help micro-pollutants adsorb to very high levels. According to Shahab Shariati et al., have been employed sodium dodecyl sulfate-modified Fe_3O_4 NPs as an effective adsorbent material to remediation cationic dyes from aqueous solutions [44]. Wenjing Guo and others [45] explained that the adsorbent coated with cetyl pyridinium chloride (CPC) on Fe-MNPs is effective at removing Sb(V). Cetylpyridinium chloride's surface modification of these nanoparticles did not alter their microstructure or morphology, as demonstrated by this study, and the particle sizes were approximately 5–10 nm. It was discovered that Fe-MNPs@CPC nanoparticles adsorb Sb(V) appropriately. In most types of waters, Fe-MNPs@CPC removed Sb(V) at rates greater than 90%, with a 99.71% removal rate in well water. Another biological substance that has been reported as a raw material for water treatment is lignin. Wang and others [46] reported that lingo-sulfonate, a surfactant derived from lignin, was used as a stabilizer in the production of magnetite nanoparticles with sizes between 100 and 200 nm. Congo-Red and titan yellow dyes, with maximum adsorbance capacities of 198.24 and 192.51 $mg.g^{-1}$, respectively, were found to adhere well to these magnetic nanoparticles. COD is an important metric for determining the amount of organic matter in wastewater, particularly from natural wastewater treatment systems [47-53]. Magnetite nanoparticles reduced detergents and chemical oxygen demand (COD) from real wastewater samples taken from three different locations of a wastewater treatment plant, while reducing total nitrogen, phosphates, and the majority of the heavy metals tested (cobalt, lead, zinc, copper, and chromium) in a high to moderate manner [54].

This study aims to determine whether nanoparticles may be used to create wastewater treatment systems that are highly effective and require less energy. Magnetite nanoparticles were chosen for this study for two primary reasons: first, they don't have any hazardous effects, and second, you can use their magnetic qualities to separate them from water more easily by using an external magnetic field. Magnetite nanoparticles were functionalized with some chemicals that served as a shell to guard against oxidation and interaction with water contaminated with a variety of contaminants. Given that organic materials make up the bulk of wastewater contaminants, Chemical Oxygen Demand (COD) was chosen as a metric of pollutants in wastewater.

2. EXPERIMENTAL

2.1. Materials

Ferric chloride anhydrous ($FeCl_3$) is prepared from Merck (Darmstadt,Germany), hydrochloric acid is prepared from(Riedel- de Haën), sodium hydroxide (NaOH) was prepared from(Fisher) Sodium lauryl ether sulfate 70% (LESTAL -270) was prepared from union chemicals factory (UCF) , was prepared from Echo chem., iron wires, black tea from Lipton and filter paper (Gf1-047). All Solutions were prepared with distilled water.

2.2. Synthesis of Fe_3O_4 NPs

Using a chemical co-precipitation method Fe_3O_4 NPs were synthesized. 0.28 M of ferric chloride was prepared by dissolving 45.42 mg of ferric chloride and 52.2 grams of iron wire in 197.8 HCl (37%). 2M sodium hydroxide solution was prepared. Boil the mixture to remove dissolved oxygen, which can cause the resultant Fe_3O_4 oxidized into Fe_2O_3, and then add NaOH solution to the mixture until the pH until the pH reaches to 10.5, then a black precipitate of magnetite particles. The formed magnetite was collected by permanent magnet and washed by boiled water for three times. The reaction was carried according to the following equation:

$$Fe^{2+} + 2Fe^{3+} + 8OH^- \rightarrow Fe_3O_4 + 4H_2O \quad (2)$$

2.3. Coating with Coconut diethanol amide (CDEA)

2 gm of CDEA (c.f. Fig. 1) was added to 500 ml of magnetite (pH of mixture is 9) and boil for 2 hours(supply the mixture with 200 ml of distilled water along the reaction time to compensate the evaporated water) collect by magnet and wash several times with distilled water then dry at 105 ^oC.

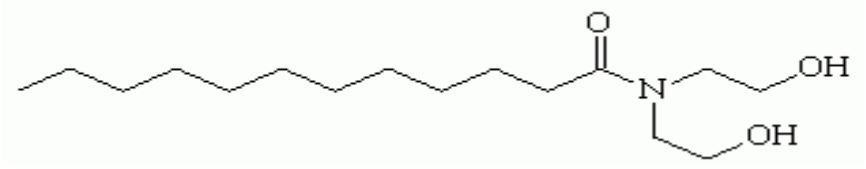

Fig. 1. Chemical structure of coconut diethanolamide

2.4. Coating with sodium lauryl ether sulfate (SLES)

2 gm of SLES (c.f. Fig. 2) was added to 500 ml of magnetite (pH of mixture is 9) as the same recipe for coating with CDEA.

Fig. 2. Chemical structure of SLES

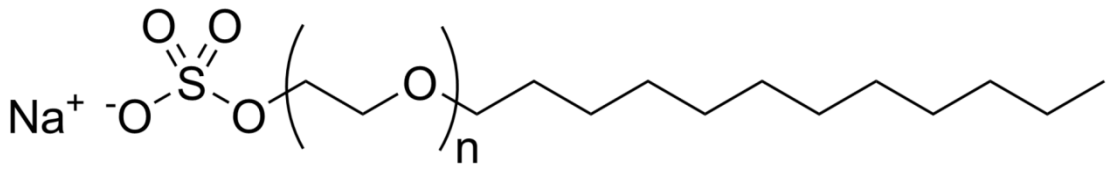

2.5. Coating with Tea (polyphenols of tannins)

Dissolve 20 gm of Lipton black tea (c.f. Fig. 3) in 500 ml of distilled water. The resulted solution was boiled to remove dissolved oxygen. Magnetite particles was added to tea solution and then boiled for 2 h to compensate the evaporated water.

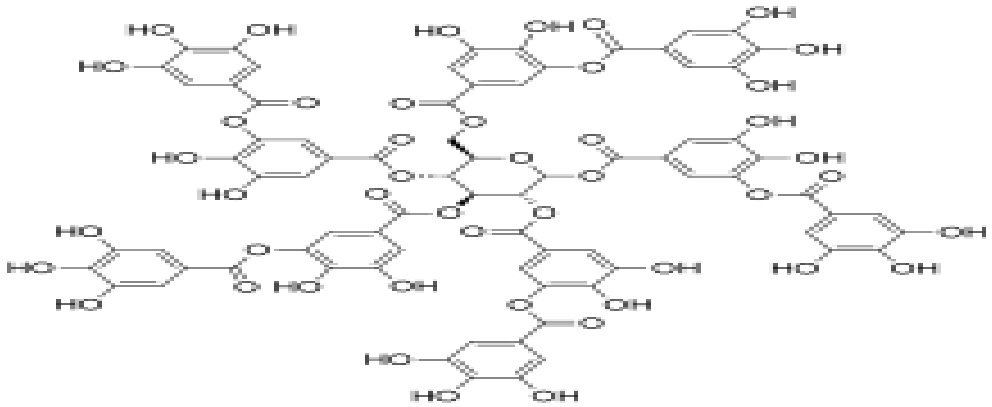

Fig. 3. Chemical structure of tannic acid

It is obvious from three structures that the function groups of these materials were different.

2.2 Techniques

On a Bruker diffractometer, X-ray diffractograms of several substances has been prepared were captured (Bruker D 8 advance target). CuK second monochromator (R = 1.5405) was used to run the patterns at 40 kV and 40 mA. A scanning rate of 8o for the phase identification and 0.8o for the line broadening profile analysis was successfully accomplished. The Scherrer eq. 3 [55] was used to measure the crystallite size of the phases found in the prepared solids:

$$d = K \lambda / \beta 1/2 \cos \theta \quad \ldots\ldots\ldots\ldots \quad (3)$$

where β1/2 is the full width at half maximum (FWHM) of the principal diffraction peaks of the present crystalline phases, θ is the diffraction angle, d is the mean crystalline diameter, X is the X-ray wavelength, K is the Scherrer constant (0.89), and d is the mean crystalline diameter. JEOL-SEM scanning electron microscope was used to investigate the surface features (SEM). By using a Quantachrome AS1WinTM-automated gas-sorption system to physically adsorb nitrogen gas at 350 °C, the surface activity of the samples was assessed (USA). The materials were degassed at 200 °C for two hours before to each sorption measurement. The samples' adsorption was utilized to determine the particular [56]. FTIR spectra of the solids were carried out empolying Shimadzu Prestige-21spectrometer on KBr discs. All of pH measurements were done by pH meter (Hanna – Hi2211). Sensitive balance (Radwag AS270/c/2) is used for weighting Fe, $FeCl_3$, SLES, CDEA and tea .Magnetic separation was done by permanent magnet. Drying oven (Thelco /precision) is used for drying the prepared sample. Distilled water apparatus (HAMILTON -WSB/4) is used for water distillation. Heater (CIMARE3-HP47130) and Magnetic stirrer (Dinko D-11) are used. As stated in our earlier research [48-53], chemical oxygen demand (COD) was utilised to assess the wastewater before and after the photocatalysis procedure in accordance with the Standard Procedures for Water and Wastewater Analysis (APHA, AWWA, 1995).

3. Results and discussion

3.1. XRD investigation

Fig. 4 shows the XRD diffraction pattern of the prepared solids. Investigation of Fig. 4 shows that;

the magnetite crystal with a characteristic peaks (2 2 0), (3 1 1), (4 0 0), (4 2 2), (5 1 1) and (4 4 0) with a cubic spinel structure (JCPDS file PDF no.65-3107). The absence of diffraction peaks at (1 1 3), (2 1 0), (2 1 3) and (2 1 0) are the characteristic peaks belong to maghemite and hematite, respectively [57]. This confirms that no other iron compounds in the obtained magnetite. In comparison of the magnetite nanoparticles with the coated samples, the diffraction peaks of XRD patterns do not change. The result obtained might indicate that the crystal structure of the magnetite nanoparticles does not considerably influenced by the coating agent. On the other hand, the degree of crystallinity was strongly dependent on the treatment. The degree of crystallinity was 13.5, 20.6, 25.5 and 27.3 a.u., for Fe_3O_4, magnetite treated with arginine, treated with tannic acid and sample treated with SLES, respectively. The calculation of the crystallite size via employing the Scherrer equationof pure magnetite, magnetite treated with arginine, treated with tannic acid and sample treated with SLES were 12.4, 15.9, 15.3 and 15 nm, respectively. Thus, we can deduced that the crystallite size significantly affected by coating agent.

3.2. Scanning Electron Microscope (SEM)

The structure of different solids of both pure and functionalized can be investigated by scanning electron microscope (SEM). Fig. 5 shows widely size-distributed and disorganized particles. As seen, the surface morphology of Fe_3O_4 is a rough with irregular size of particles. Upon coating, this surface was well-covered by the studied modifiers exhibiting the successful route of modification.

3.3. FT-IR Investigation

Fig. 6 show FT-IR spectra of pure Fe_3O_4 and coated samples. Investigation of Fig. 6 revealed that the stretching vibration bands around 3400 and 1630 cm^{-1} express the vibration of H_2O still present in the samples and bands in 570 and 468 cm^{-1} which is the representative absorption bands of the Fe-O bond of bulk Fe_3O_4 [58].

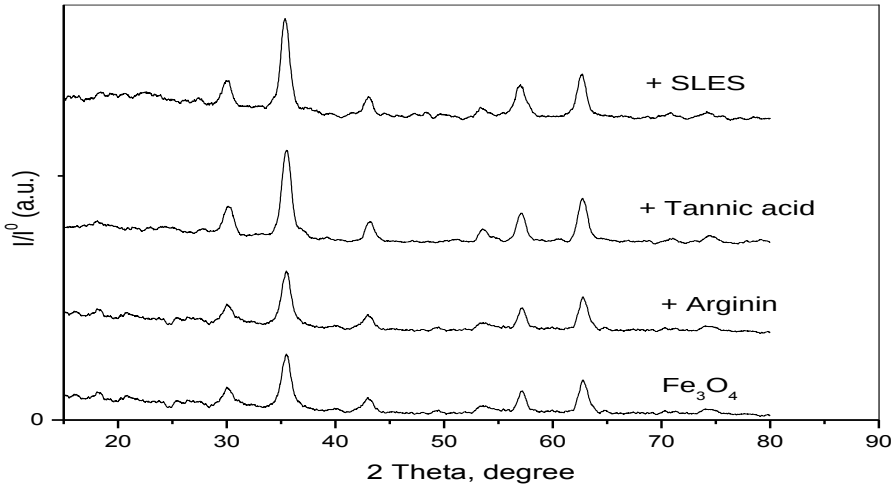

Fig. 4. XRD patterns of prepared samples

A deep investigation of Fig. 3 reveals that the bands related to the Fe-O bond (in 570 and 468 cm^{-1}, respectively) were displaced to high wavenumbers of around 600 and 490 cm^{-1}. Additionally, the band near 600 cm^{-1} split, was producing the bands in 631.4 and 582.9 cm^{-1}. This might be explained by the fact that the breakdown of bonds caused the inlocalized electrons on the particle surface to rearrange, leading to the development of finite size [59].

3.4. Texture properties of the prepared solids

N_2 adsorption/desorption isotherms of the prepared solids were represented in Fig. 7**.** The isotherm graphs of all prepared solids indicate to type IV of H3 hysteresis loop in which a relative pressure P/P^o increase > 0.75. The increase of relative pressure might be attributed to the capillary condensation of the solids. Investigation of Fig. 4 revealed that the modification of NPs increase pore diameter and mesopore volume. These results reflect that SLES and tannic might be mesoporous agent for NPs. The total pore volume of the synthesized solids is shown in Table 1 together with the computed S_{BET}. The data from Table 1 demonstrated the treatment of the sample have obvious effect on total pore volume.

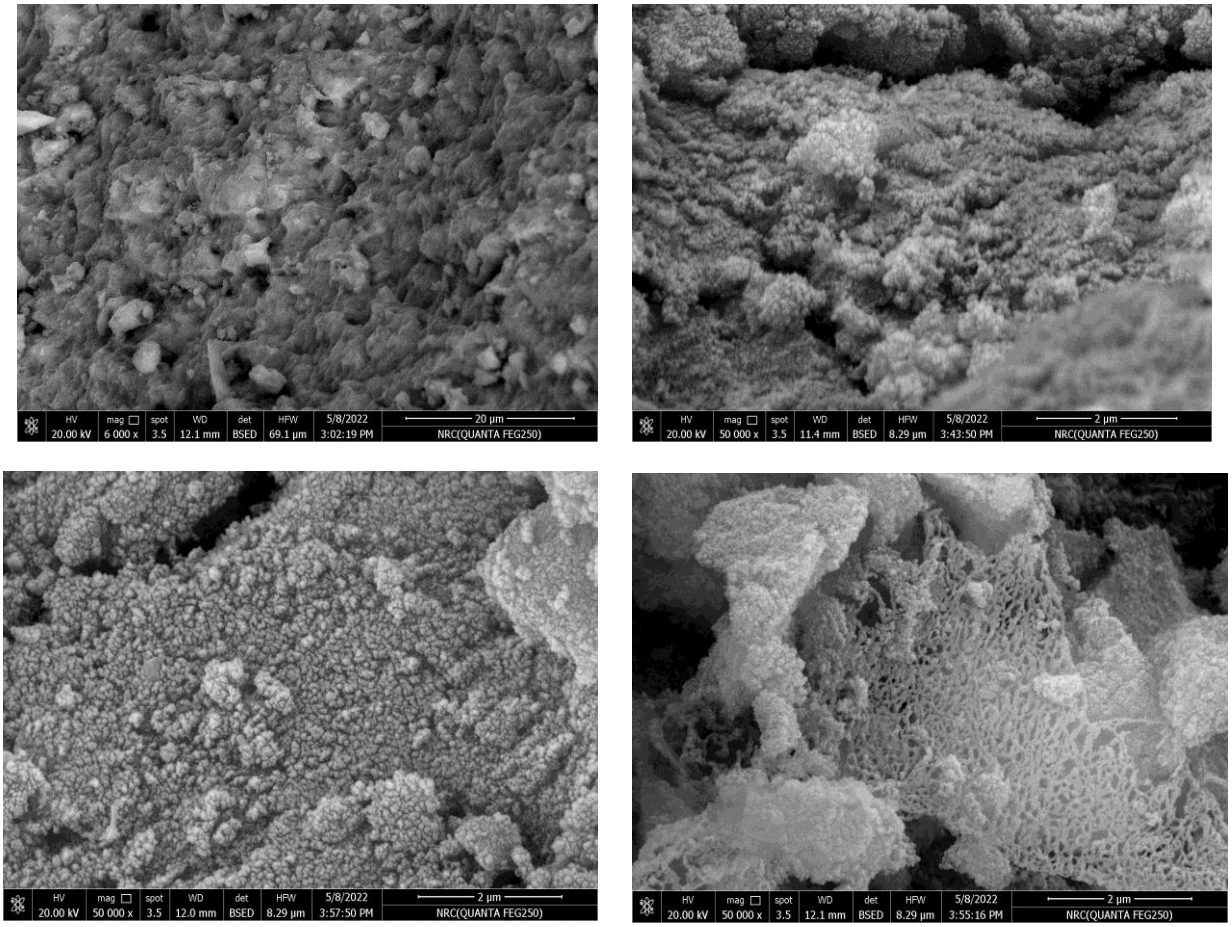

Fig. 5. Scanning electron microscope (SEM) images of (a) pure, (b) treated by arginine (c) treated by tannic acid (d) treated by SLES

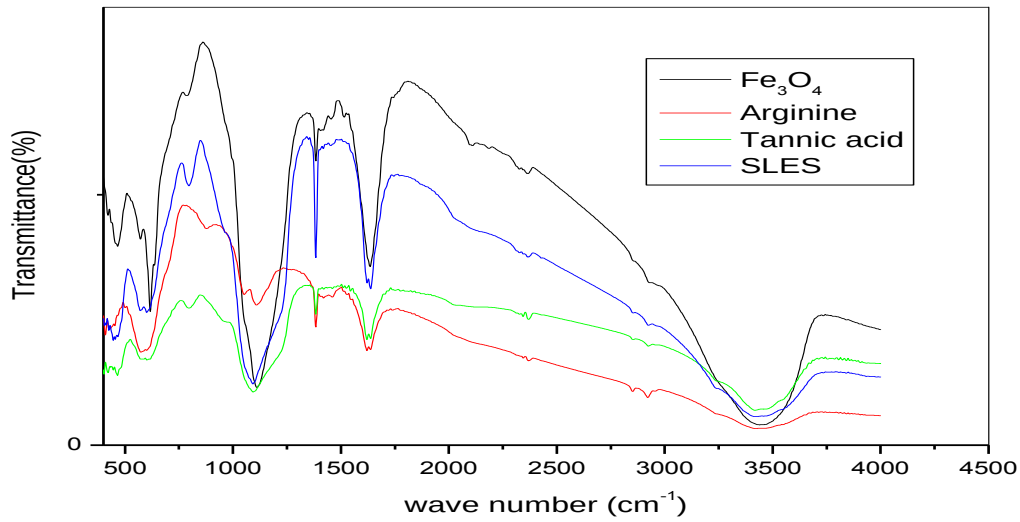

Fig. 6. FTIR spectra for magnetite nanoparticles

Fig. 7. N_2- adsorption-desorption isotherm of different prepared samples

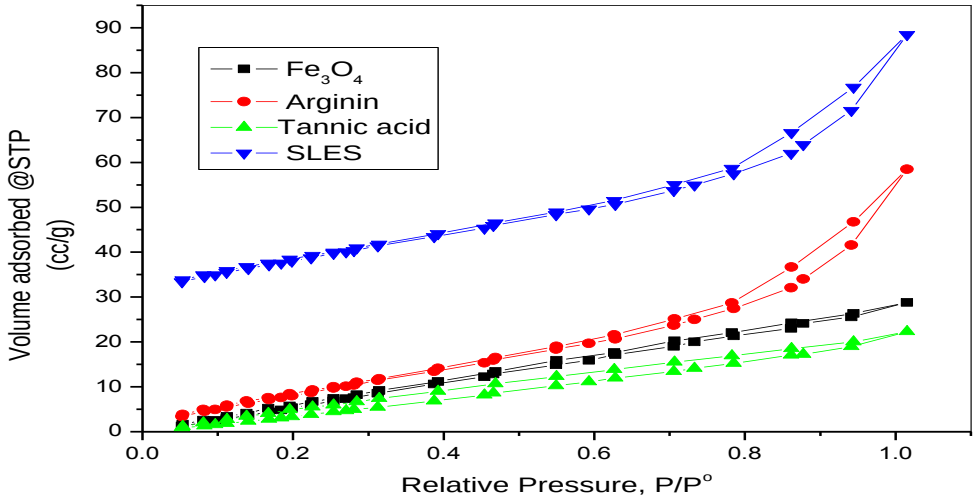

Table 1: Surface characteristics of the prepared solids

Solid	$S_{BET,}$ m^2/g	Total pore volume Vp , cm^3/g	Mean pore radius r^- (nm)
Fe_3O_4	32.38	0.05036	3.11
+ Arginin	35.24	0.0345	1.96
+ Tannic acid	42.05	0.0907	4.31
+ SLES	54.35	0.0447	1.64

As a result, treatment NPs both increase surface area and reduce pore size. Therefore, the treated solids may serve as effective organic pollutant adsorbents.

3.5. Catalytic degradation

The photocatalytic activity under sunlight of the synthesized samples for catalytic degradation of organic pollutant from wastewater supplied from Tafahna station (Gharbia governorate, Egypt) after primary precipitation. The samples have low degradation activity by carrying out the experiments without primary precipitation.

However, the catalytic activity was remarkably improved by carrying out primary precipitation (c.f. Fig. 8). All samples recorded photocatalytic activity towards degradation of organic pollutants; however the solids of Fe_3O_4@SLES showed the highest activity referring that increasing the functional groups in SLES has a positive role in the oxidation of organic pollutants. This refers that by increasing the functional groups increasing the efficiency of oxidation as it is enhanced the electron transfer and inhibits the electron-hole pairs recombination. So, our study reported that the presence of multi-function groups which display a different active sites for adsorption which represents a synergetic factor for photo-catalysis process. The relatively higher catalytic role of this sample might be attributed to the coexistence of Fe_3O_4 and multi-functional groups.

These results lead us to conclude that catalytic activity is related to the presence of function groups and their type present in the sample, and Fe_3O_4@SLES is an efficient catalyst for organic pollutant degradation. On the other hand, in case of Fe_3O_4@tannic acid and Fe_3O_4@Arginin a clear decrease of organic pollutant removal efficiency (83% and 64%, respectively) was observed as indicated in Fig. 8.

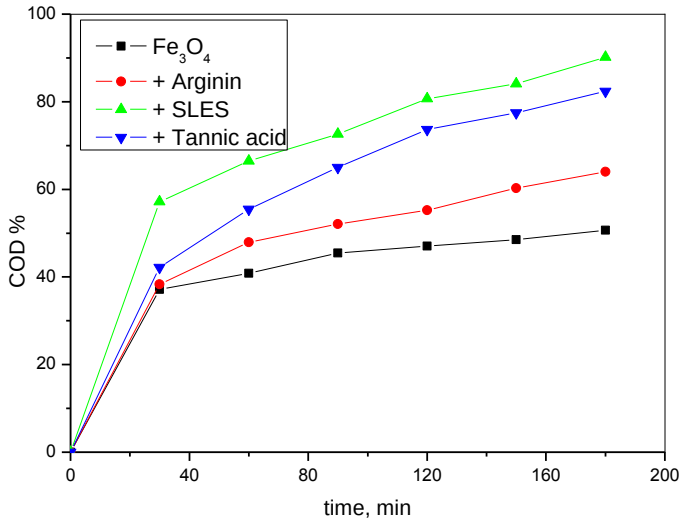

Figure 8. Organic pollutant degradation activity of various prepared solids at different degradation time

The decrease in organic pollutant degradation was due to the fewer available active site on their surfaces or due to the steric of these function groups as shown in tannic acid (c.f. Fig. 3, section 2.5.).

A possible catalytic mechanism could be assigned to that irradiation of the synthesizes catalysts by sunlight leads to establishment of free active oxygen species: $OH^{\bullet}$, $O_2^{\bullet-}$, and $H_2O^{\bullet-}$ radicals. The presence of SLES accompanied with Fe_3O_4 structure led to an increase in the functional group with catalytically active interfaces. Eqs (4-7) represent a possible course for the boosted catalytic degradation of Fe_3O_4@SLES sample against organic compounds. The produced samples' increased interface contact makes it easier for electrons and holes to move between the conduction and valence bands of FeO and Fe_2O_3, respectively. A more efficient interelectron transfer occurs between the catalyst's components as a result of the creation of such heterojunction. This separated the photo-induced electron-hole pairs and decreased the likelihood of electron-hole pairs recombining, which is essential for the photocatalytic reaction.

$Fe_3O_4 + \lambda v \rightarrow Fe_3O_4(é) + Fe_3O_4(h^+)$ (4)

$Fe_3O_4(é) + O_2 \rightarrow Fe_3O_4 + O_2^{\cdot-}$ (5)

$Fe_3O_4(h^+) + OH^- \rightarrow Fe_3O_4 + OH^{\cdot}$ (6)

Organic compound $+ O_2^{\cdot-} \rightarrow CO_2 + H_2O$ (7)

4. Conclusions

Fabrication of Fe_3O_4 has been achieved by employing coprecipitation method. Treating the prepared Fe_3O_4 by CDEA, Tannic acid and SLES was carried out. The XRD displays that the highest intensity peaks were at 2θ=34.87°, which related to the reflection plane (400) and referred to the major peak of Fe_3O_4 crystallites. The average crystallite size of Fe_3O_4 nanoparticles was found to be 15 ±3 nm. The results of SEM revealed that the sample containing widely size-distributed and disorganized particles. Textural investigation revealed that the modification of NPs increase pore diameter and mesopore volume. All samples recorded photocatalytic activity towards degradation of organic pollutants; however the solids of Fe_3O_4@SLES showed the highest activity referring that increasing the functional groups in SLES has a positive role in the oxidation of organic pollutants. The order of photocatalytic activity was Fe_3O_4@SLES > Fe_3O_4@tannic acid > Fe_3O_4@arginin > Fe_3O_4. These modifiers could enhance the photocatalytic activity of Fe_3O_4 by decreasing its band gap energy and thus absorption efficiency and adsorption capacity was increased as a result of increase in total surface area and adsorption active sites.

Conflict of interest

The authors have declared that there is no a conflict of interest.

References

[1] Pirsaheb M, Khamutian R, Khodadadian M, A comparison between extended aeration sludge and conventional activated sludge treatment for

removal of linear alkylbenzene sulfonates (case study: Kermanshah and Paveh WWTP). Desalin Water Treat, 2014. 52(25–27): p.4673–4680.

[2] Collins AL, Newell Price JP, Zhang Y, Gooday R, Naden PS, Skirvin D, Assessing the potential impacts of a revised set of on-farm nutrient and sediment 'basic' control measures for reducing agricultural diffuse pollution across England. Sci Total Environ., 2018. 621, p.1499–1511.

[3] De Andrade J.R., Oliveira M.F., Da Silva MGC, Vieira MGA. Adsorption of pharmaceuticals from water and wastewater using nonconventional low-cost materials: A review. Industrial and Engineering Chemistry Research. 2018.57(9), p.3103-3127

[4] Carlos F.S., Schaffer N., Andreazza R, Morris L.A., Tedesco M.J., Boechat C.L., et al. Treated industrial wastewater effects on chemical constitution maize biomass, physicochemical soil properties, and economic balance. Communications in Soil Science and Plant Analysis, 2018. 49(3), p.319-333.

[5] Juang R.S. , WuF.C. , TsengR.L. , Characterization and use of activated carbons prepared from bagasse for liquid-phase adsorption, Colloids Surf., A ,2002. 201, p. 191–199.

[6] A. Mirsha, M. Bajpaj, The flocculation performances of Tamarindus Mucilage in relation to removal of vat and direct dyes, Bioresour. Technol. 2006. 97, 1055–1059.

[7] Aleboyeh A., Aleboyeh H., Effects of gap size and UV dosage on decolorization of C. I. Acid Orange 7 by UV/H_2O_2 process, J. Hazard. Mater. 2006. 133, p. 167–171.

[8] Liao M.H., Chen D.H., Fast and efficient adsorption/desorption of protein by a novel magnetic nano-adsorbent, Biotechnol. Lett. 2002. 24, p. 1913–1917.

[9] Yang N., Zhu S., Zhang D., Xu S., Synthesis and properties of magnetic Fe_3O_4- activated carbon nanocomposite particles for dye removal, Mater. Lett. 2008. 62, p. 645–647.

[10] Liao M.H., Wu K.Y., Chen D.H., Fast removal of basic dyes by a novel magnetic nano-adsorbent, Chem. Lett. 2003. 6,p. 488–489.

[11] Wang L., Yang Z., Gao J., Xu K., Gu H., Zhang B., Zhang X., Xu B., A biocompatible method of decorporation: bisphosphonate-modified magnetite nanoparticles to remove uranyl ions from blood, J. Am. Chem. Soc. 2006. 128, p. 13358–13359.

[12] Faraji M., Yamini Y., Saleh A., Rezaee M., Ghambarian M., Hassani R., A nanoparticle-based solid-phase extraction procedure followed by flow injection inductively coupled plasma-optical emission spectrometry to determine some heavy metal ions in water samples, Anal. Chim. Acta, 2010. 659, p. 172–177.

[13] Li P., Miser D.E., Rabiei S., Yadav R.T., Hajaligol M.R., The removal of carbon monoxide by iron oxide nanoparticles, Appl. Catal. B Environ., 2003. 43, p. 151–162

[14] Laurent S, Forge D, Port M et al, Magnetic iron oxide nanoparticles: synthesis, stabilization, vectorization, physicochemical characterizations, and biological applications. Chem Rev, 2008. 108, 2064–2110.

[15] Wu W., Wu Z., Yu T. et al, Recent progress on magnetic iron oxide nanoparticles: synthesis, surface functional strategies and biomedical applications. Sci. Technol. Adv. Mater., 2015. 16, p. 023501.

[16] Ling D., Lee N., Hyeon T., Chemical synthesis and assembly of uniformly sized iron oxide nanoparticles for medical applications. Acc. Chem. Res., 2015. 48, p.1276–1285.

[17] Roth H-C, Schwaminger SP, Schindler M. et al, Influencing factors in the CO-precipitation process of superparamagnetic iron oxide nano particles: a model based study. J. Magn Magn Mater, 2015. 377, p.81–89.

[18] Pušnik K., Goršak T., Drofenik M., Makovec D. Synthesis of aqueous suspensions of magnetic nanoparticles with the co-precipitation of iron ions in the presence of aspartic acid. J Magn Magn Mater, 2016, 413, p. 65–75.

[19] Lin S., Lin K., Lu D., Liu Z., Preparation of uniform magnetic iron oxide nanoparticles by co-precipitation in a helical module microchannel reactor. J. Environ. Chem. Eng., 2017. 5, p.303–309.

[20] Cheng W., Xu X., Wu F., Li J., Synthesis of cavity-containing iron oxide nanoparticles by hydrothermal treatment of colloidal dispersion. Mater Lett., 2016. 164, p.210–212.

[21] Gyergyek S., Makovec D., Jagodič M. et al., Hydrothermal growth of iron oxide NPs with a uniform size distribution for magnetically induced hyperthermia: structural, colloidal and magnetic properties. J. Alloys Compd., 2017. 694, p. 261–271.

[22] Bhavani P., Rajababu C.H., Arif M.D. et al., Synthesis of high saturation magnetic iron oxide nanomaterials via low temperature

hydrothermal method. J. Magn. Magn. Mater., 2017. 426, p.459–466.
[23] Girginova P.I., Daniel-da-Silva A.L., Lopes C.B. et al., Silica coated magnetite particles for magnetic removal of Hg^{2+} from water. J. Colloid Interface Sci., 2010. 345, p.234–240.
[24] Reguyal F., Sarmah A.K., Gao W., Synthesis of magnetic biochar from pine sawdust via oxidative hydrolysis of FeCl2 for the removal sulfamethoxazole from aqueous solution. J Hazard Mater, 2017. 321, p.868–878.
[25] Jiang F., Li X., Zhu Y., Tang Z., Synthesis and magnetic characterizations of uniform iron oxide nanoparticles, Phys. B Condens Matter, 2014. 443, p.1–5.
[26] Glasgow W., Fellows B., Qi B. et al, Continuous synthesis of iron oxide (Fe_3O_4) nanoparticles via thermal decomposition. Particuology, 2016. 26, p.47–53.
[27] Bartůněk V., Průcha D., Švecov M. et al, Ultrafine ferromagnetic iron oxide nanoparticles: facile synthesis by low temperature decomposition of iron glycerolate. Mater. Chem. Phys., 2016. 180, p.272–278.
[28] Sandeep K. V., Magnetic nanoparticles-based biomedical and bioanalytical applications. J Nanomed Nanotechol, 2013. 4, e130.
[29] Massart R., Cabuil V., Effect of some parameters on the formation of colloidal magnetite in alkaline-medium-yield and paricle-size control. J. Chem. Physics, 1987. 8, p. 967 - 973.
[30] Gorski C. A., Scherer M. M., Determination of nanoparticulate magnetite stoichiometry by Mössbauer spectroscopy, acidic dissolution, and powder X-ray diffraction: A critical review American Mineralogist, 2010. 95, p.1017–1026.
[31] Abdel Maksoud MIA, Elgarahy A.M., Farrell C. et al., Insight on water remediation application using magnetic nanomaterials and biosorbents. Coord. Chem. Rev., 2020. 403, p.213096.
[32] D'Cruz B., Madkour M., Amin M.O., Al-Hetlani E., Efficient and recoverable magnetic AC-Fe_3O_4 nanocomposite for rapid removal of promazine from wastewater. Mater. Chem. Phys., 2020. 240, p.122109.
[33] Hu X., Hu Y., Xu G. et al., Green synthesis of a magnetic β-cyclodextrin polymer for rapid removal of organic micropollutants and heavy metals from dyeing wastewater. Environ Res, 2020. 180, p.108796.
[34] Mittal H., Babu R., Dabbawala A.A., Alhassan S.M., Low-temperature synthesis of magnetic carbonaceous materials coated with nanosilica for rapid adsorption of methylene blue. ACS Omega, 2020. 5, p. 6100–6112
[35] Ahmad M., Wang J., Xu J. et al, Novel synthetic method for magnetic sulphonated tubular trap for efficient mercury removal from wastewater. J. Colloid Interface Sci., 2020. 565, p. 523–535.
[36] Wang G., Luo Q., Dai J., Deng N., Adsorption of dichromate ions from aqueous solution onto magnetic graphene oxide modified by β-cyclodextrin. Environ. Sci. Pollut. Res., 2020. 27, p. 30778–30788.
[37] Wang Z., Zhang J., Wu Q. et al., Magnetic supramolecular polymer: Ultrahigh and highly selective Pb(II) capture from aqueous solution and battery wastewater. Chemosphere, 2020. 248, p.126042.
[38] Jafari Z., Avargani V.M., Rahimi M.R., Mosleh S., Magnetic nanoparticles- embedded nitrogen-doped carbon nanotube/porous carbon hybrid derived from a metal-organic framework as a highly efficient adsorbent for selective removal of Pb(II) ions from aqueous solution. J. Mol. Liq, 2020. 318, p.113987.
[39] Keykhaee M., Razaghi M, Dalvand A et al, Magnetic carnosine-based metal-organic framework nanoparticles: fabrication, characterization and application as arsenic adsorbent, J. Environ. Heal Sci. Eng., 2020. 18, p.1163–1174.
[40] Icten O., Ozer D., Magnetite doped metal–organic framework nanocomposites: an efficient adsorbent for removal of bisphenol- A pollutant. New J. Chem., 2021. 45, p.2157–2166.
[41] Xin Y., Gu P., Long H. et al., Fabrication of ferrihydrite-loaded magnetic sugar cane bagasse charcoal adsorbent for the adsorptive removal of selenite from aqueous solution. Colloids Surfaces A Physicochem. Eng. Asp., 2021. 614, p.126131
[42] Tan Z., Gao M., Dai J. et al, Magnetic Interconnected macroporous imprinted foams for selective recognition and adsorptive removal of phenolic pollution from water. Fibers Polym., 2020. 21, p.762–774.
[43] Fan S., Qu Y., Yao L. et al, MOF-derived cluster-shaped magnetic nanocomposite with hierarchical pores as an efficient and regenerative adsorbent for chlortetracycline removal. J Colloid Interface Sci., 2021. 586, p.433–444.
[44] Shariati S., Faraji M., Yamini Y., Rajabi A. A., Fe_3O_4 magnetic nanoparticles modified with sodium dodecyl sulfate for removal of safranin

O dye from aqueous solutions, Desalination, 2011. 270, p. 160–165.
[45] Guo W., Fu Z., Zhang Z., Wang H., Liu S., Feng W., Zhao X., Giesy J. P., Synthesis of Fe_3O_4 magnetic nanoparticles coated with cationic surfactants and their applications in Sb(V) removal from water, Science of the total Environment, 2020. 710, p. 136302.
[46] Hu L., Guang C., Liu Y., Su Z., Gong S., Yao Y.,Wang Y., Adsorption behavior of dyes from an aqueous solution onto composite magnetic lignin adsorbent. Chemosphere 2020, 246, 125757.
[47] Pietrzyk P., Phuong N.T., Olusegun S.J., Nam N. Thanh D.T.M., Giersig M., Krysi´nski P. Osial M., Titan Yellow and CongoRed Removal with Superparamagnetic Iron-Oxide-Based Nanoparticles Doped with Zinc. Magnetochemistry 2022. 8, p. 91.
[48] Ibrahim S. M., Badawy A. A., Characterization and use for the degradation of phenol, of new coreshell mesoporous Si–Sn–Zr oxides synthesized by a surfactantassisted sol–gel self-combustion method, , J. Sol-Gel Sci. and Technol., 2022. 101, p. 453–467.
[49] Wahaba M. A., Badawy A.A., Novel Zr-Cu-Fe Nanocomposite Metal Oxides: Structural, Magnetic and Composition Activity Effects on Photodegradation of Phenols, J. sol-gel sci. Technol. 2020. 94(3), p. 637-647.
[50] Ghanem A.F. , Badawy A.A., Mohram M. E., Abd A. FelRehim M. H., Synergistic effect of Zinc oxide nanorods on the photocatalytic performance and the biological activity of graphene nanosheets, Heliyon, 2020. 6, p. e03283.
[51] Al-Harby N.F., A. A. Badawy, Ibrahim S. M., Improvement of Nanosized CuO-Fe_2O_3/ cordierite System by Li_2O-treatment for wastewater treatment, , J. Ultrafine Grained and Nanostructured Materials, 2019. 52 (2), p. 175-187.
[52] Ghanem A. F., Badawy A. A., Mohram M. E., Abdelrehim M.H., Enhancement the Photocatalytic and Biological Activity of Nano-sized ZnO Using Hyperbranched Polyester, J. of Inorganic and Organometallic Polymers and Materials, 2019. 29, 28–938.
[53] Abdel Rehim M. H., El-Samahy M. A., Badawy A.A., Mohram M. E., Photocatalytic activity and antimicrobial properties of paper sheets modified with TiO_2/Sodium alginate nanocomposites, Carbohydrate Polymers, 2016. 148, p. 194–199.
[54] Castelo-Grande T, Augusto P.A., Rico J. et al., Magnetic water treatment in a wastewater treatment plant: Part I - sorption and magnetic particles. J. Environ. Manage, 2021. 281, p. 111872.
[55] Cullity, B.D.: Publishing Cos, 2nd edn, p. 102. Addison-Wesley, Boston (1978)
[56] Rouquerol J., Rouquerol, F., Llewellyn P., Maurin G., Sing K. S. (2013). Adsorption by powders and porous solids: principles, methodology and applications. Academic press.
[57] Jang J.H., Lim H.B., Characterization and analytical application of surface modified magnetic nanoparticles, Microchem. J., 2010. 94, p. 148–158.
[58] Bui T.Q., Ton S. N-C., Duong A.T., Tran H. T., Size-dependent magnetic responsiveness of magnetite nanoparticles synthesised by co-precipitation and solvothermal method, / J. Sci.: Advanced Mat. and Devices, 2018. 3, 107-112.
[59] Abobakr S. M., Abdo N. I., Adsorption Studies on Chromium Ion Removal from Aqueous Solution Using Magnetite Nanoparticles, Egypt. J. Chem. 2022. **65**, 21 – 29.